Journal of *Marine Science and Engineering*

MDPI

Article

Storm-Driven Geomorphological Changes on a Mediterranean Beach: High-Resolution UAV Monitoring and Advanced GIS Analysis

Marco Luppichini

Department of Earth Sciences, University of Pisa, via Santa Maria 53, 56121 Pisa, Italy; marco.luppichini@dst.unipi.it

Abstract

Coastal erosion is a growing concern in the Mediterranean region, where the combined effects of anthropogenic pressure, reduced fluvial sediment supply, and climate change-driven sea level rise and extreme storm events threaten the stability of sandy shorelines. This study examines the geomorphological impacts of the exceptional storm surge of 3 November 2023, associated with Storm Ciaran, which affected a vulnerable coastal segment north of the Morto Nuovo River in northern Tuscany (Italy). Using UAV-based photogrammetric surveys and high-resolution morphological analysis, we quantified shoreline retreat, dune toe regression, beach slope changes, and sediment volume loss. The storm induced an average shoreline retreat of over 5 m, with local peaks reaching 30 m, and a dune toe setback of up to 7 m. A net sediment budget deficit of approximately 1800 m^3 was recorded, over 50% of the total volume added during soft nourishment interventions performed in the previous decade. Our findings highlight how a single high-energy event can match or exceed the annual average erosion rate, emphasizing the limitations of traditional shoreline-based monitoring and hard defense structures. This study highlights the importance of frequent, high-resolution monitoring focused on individual storm events, which is crucial to better understand their specific geomorphological impacts. Such detailed analyses help clarify whether long-term erosion trends are primarily driven by the cumulative effect of high-energy events. This knowledge is essential for identifying the most effective coastal protection strategies and for improving the design of defense structures. This approach is particularly relevant in the context of climate change, which is expected to increase the frequency and intensity of extreme events, making it imperative to base future planning on accurate, event-driven data.

Keywords: coastal erosion; storm surge; UAV photogrammetry; morphodynamic response; sediment budget

check for updates

Academic Editors: Chatzipavlis Antonis and Simone Simeone

Received: 10 July 2025
Revised: 11 August 2025
Accepted: 14 August 2025
Published: 15 August 2025

Citation: Luppichini, M. Storm-Driven Geomorphological Changes on a Mediterranean Beach: High-Resolution UAV Monitoring and Advanced GIS Analysis. *J. Mar. Sci. Eng.* **2025**, *13*, 1568. https://doi.org/10.3390/jmse13081568

Copyright: © 2025 by the author. Licensee MDPI, Basel, Switzerland. This article is an open access article distributed under the terms and conditions of the Creative Commons Attribution (CC BY) license (https://creativecommons.org/licenses/by/4.0/).

1. Introduction

Coastal erosion represents one of the most critical environmental challenges globally [1], and within this context, the Mediterranean region emerges as an area particularly vulnerable to the effects of climate change [2–4] and coastal erosion [5]. The Mediterranean coastal system is inherently fragile due to the combined effect of intense anthropogenic pressures [6–8] and the growing influence of climate-related drivers [1,9]. The interaction between reduced fluvial sediment supply, rising sea levels, and the increasing frequency and intensity of extreme events contributes to the progressive weakening of the resilience of sandy coastal areas, especially near river deltas [5,10–12].

In the Italian context, many coastal stretches display long-term erosion trends, documented by extensive historical datasets, with shoreline retreat rates in some cases exceeding 5–6 m per year [13–21]. The coastal plain of Pisa, in particular, has long been identified as an erosion hotspot, with morphodynamic processes heavily influenced by the limited sediment supply from the Arno River [22–27] and by the action of storm waves from the SW and NW quadrants [28–30].

Studies on coastal erosion often focus on the shoreline evolution and associated retreat rates, which are essential to identify the most erosion-prone areas and, in some cases, to infer underlying causes. The diachronic analysis of shoreline position allows researchers to correlate morphological changes to human interventions both along the coast and inland, such as dam construction or riverbed sediment mining [6].

The evolution of the coastal zone is traditionally monitored using direct observation techniques (e.g., DGPS surveys, UAV photogrammetry, and detailed topography) [21,31–38] and remote sensing methods (e.g., multispectral satellite imagery and historical cartography), which enable the reconstruction of geomorphological trends over extended temporal scales [39–46].

However, an increasingly relevant aspect in coastal studies concerns the understanding of morphological responses to individual extreme events, such as intense storm surges [47]. These events can trigger changes in the subaerial beach profile comparable to, or even exceeding, those accumulated over years of regular morphodynamic activity, rapidly reshaping the coastline and exposing previously stable sectors to risk.

In the context of climate change, with more frequent and intense extreme events expected [1,48,49], the ability to analyze the localized morphological impacts of individual storms becomes essential to improve forecast scenarios and guide more effective coastal management strategies.

This study aims to contribute to the understanding of the geomorphological impacts produced by a single exceptional meteomarine event, the storm surge of 3 November 2023, associated with Storm Ciaran, which affected a particularly vulnerable stretch of the Italian coastline. The focus is on a 500 m coastal segment north of the Morto Nuovo River, within the littoral cell between the Scolmatore Channel and the Magra River in northern Tuscany.

The objective is to quantify the geomorphological effects of the extreme event by measuring elevation changes, sediment volume loss, and shoreline retreat along this highly sensitive coastal sector, in order to improve the understanding of morphodynamic responses to impulsive events and to provide useful elements for the enhancement of management and adaptation strategies for vulnerable coastal zones.

2. Study Area

The study area is located along the central coast of Tuscany (Figure 1), within the Migliarino San Rossore Massaciuccoli Regional Park, and corresponds to a coastal stretch of approximately 500 m immediately north of the reinforced mouth of the Morto Nuovo River, a watercourse forming part of the land reclamation system of the Pisan plain, established in 1864. This coastal sector, situated between the mouths of the Arno River (to the south) and the Serchio River (to the north), develops along a sandy shoreline with high natural value, preserved through the environmental protection provided by the park authority.

The coastal stretch is characterized by a sandy beach with a generally straight profile and north–south orientation. Inland, a well-developed system of beach ridges extends for several kilometers, formed, like the rest of the Pisan coastal plain, since Etruscan times [50–53]. In some places, these ridges are overlain by coastal dunes [50], which are now interrupted by ongoing erosional processes that, over the past 150 years, have reversed

the long-term progradation trend that had shaped this stretch of coast since the Etruscan period [28–30,54–57].

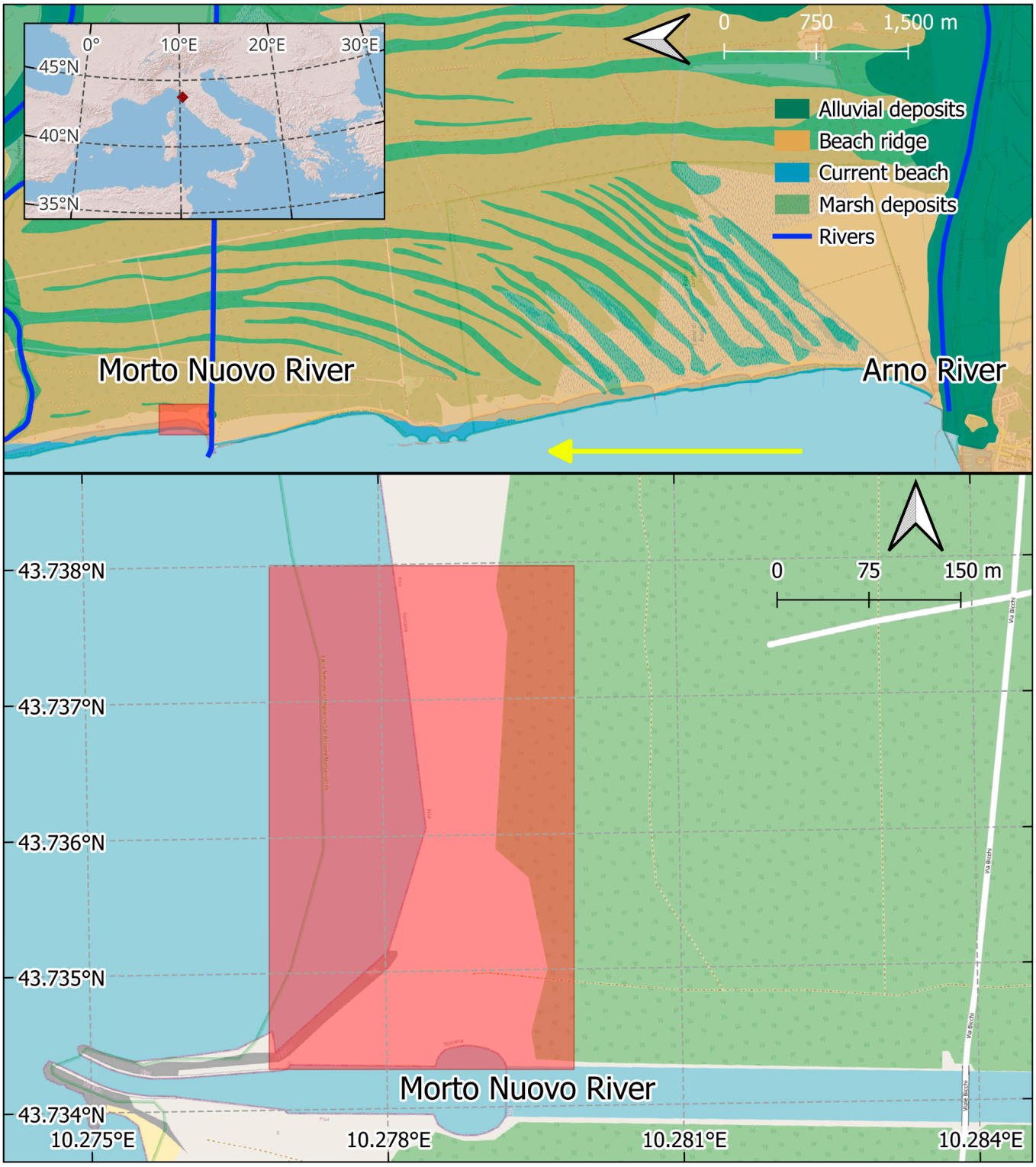


Figure 1. Geographic and geomorphological context of the Morto Nuovo River mouth area. The upper panel shows the distribution of current beach, alluvial deposits, beach ridge systems, and marsh deposits, highlighting the progradation history of the Arno delta. The yellow arrow indicates the direction of the long-shore current. The lower panel shows a high-resolution satellite image with the study area outlined in red, where the storm impact assessment was conducted.

The area is located in a microtidal environment, with a mean tidal range not exceeding 30 cm, and is highly exposed to storm events from the southwest (Libeccio winds), which are the dominant direction of high-energy wave events in this part of the Ligurian Sea [26]. Along this sector, the longshore sediment transport is directed northward and has historically been fed primarily by sediments from the Arno River [58].

In this context, the natural sediment supply that had supported the progradation of the coastal plain since the Etruscan era has been drastically reduced due to progressive alterations in the Arno River catchment during the 20th century, including the intensification of river regulation works, the construction of dams, and the sharp reduction in sediment load [22,23,27]. As a result, coastal erosion began to prevail from the early 20th century onward.

The area is not subject to significant tourist flows, and thanks to the protection efforts of the park authority, human impact is limited to hydraulic engineering interventions, such as the construction of the Morto Nuovo River in 1864 and a series of coastal defense structures. In particular, the mouth of the Morto Nuovo River was reinforced in 1933 and later integrated with shore-parallel barriers in 2011.

The study area is thus characterized by a high degree of naturalness, supported by the absence of permanent infrastructure and low anthropogenic pressure. However, it is important to acknowledge the presence of historical modifications linked to land reclamation and hydraulic management activities, such as the construction of the Morto Nuovo River and the subsequent coastal defenses. Despite these interventions, the coastal tract remains a relatively unaltered environment, making it especially suitable for the analysis of morphodynamic responses to high-energy natural events under quasi-natural conditions.

3. Materials and Methods

3.1. Topographic Surveys and Morphological Analysis

Photogrammetric data acquisition was carried out through two UAV flights planned with the objective of generating high-resolution products suitable for morphological assessment of the coastal zone. The UAV flight missions were conducted on 19 June 2023, between 14:45 and 15:30 UTC, and on 6 November 2023, between 15:20 and 15:40 UTC. According to tide gauge data from the IOC–Sea Level Monitoring station at Livorno (LI11) [https://www.ioc-sealevelmonitoring.org/station.php?code=LI11 (accessed on 8 August 2025)], the sea level during the June survey was approximately −0.2 m, while during the November survey it was approximately +0.2 m. The surveys were performed using a DJI Phantom 4 Pro V2 drone, flying at a planned altitude of 40 m above ground level, with high longitudinal and transverse overlap (greater than 80%) and equipped with an 8.8 mm FC6310S camera. Data acquisition was conducted under diffuse lighting conditions and in the absence of wind to minimize shadows and geometric distortions. The survey was supported by Ground Control Points (GCPs) measured in the field using a differential GNSS Emlid Reach RS2 system, operating in RTK mode. The number of GCPs used exceeded 10, in accordance with the methodological recommendations proposed by [59].

The acquired images were processed using Agisoft Metashape Professional software, following a standard workflow: image alignment, optimization with GCPs, dense point cloud generation, and the creation of both the Digital Elevation Model (DEM) and the orthomosaic.

To ensure the geometric accuracy of the outputs, GCPs were distributed evenly across the entire survey area [59] and validated using a variable number of check points. The resulting models were exported to a GIS environment for spatial analysis.

Shoreline extraction was performed using the method proposed by [38], which involves the automated detection of the intersection between beach and sea, based on the slope gradient derived from the DEM. The dune toe position was instead determined

using the Sky-View Factor (SVF), calculated from the DEMs. The SVF is an indicator of the portion of visible sky from each surface point and is computed as the integral of hemispherical visibility, with values ranging from 0 (fully obstructed) to 1 (fully open). In coastal geomorphology, the SVF is useful for detecting topographic transitions, such as the shift from beach to dune base, which appears as a sharp contrast from high to low SVF values. This discontinuity was used to map the dune toe position along cross-shore transects, combining elevation data with threshold analysis in a GIS environment.

Elevation changes between the two surveys were calculated by resampling the November DEM to match the grid of the June DEM, ensuring precise spatial correspondence. The analysis was performed using map algebra, applying a pixel-by-pixel subtraction between the elevation values. Positive values indicate accretion, while negative values indicate erosion.

Slope variations were estimated along cross-shore transects spaced approximately every 5 m. For each profile, slope values were calculated from the DEMs of both surveys and compared in terms of absolute variation.

All spatial analyses, including displacement statistics and volume calculations, were performed in QGIS or using Python v3.11 scripts developed with the Geopandas GIS library.

3.2. Meteo-Oceanographic Data: RON Buoy and ERA5 Reanalysis

To reconstruct the meteomarine evolution of the 3 November 2023 event, an integrated methodology was adopted, combining in situ observational data with atmospheric reanalysis model outputs.

The marine component was analyzed using data from the National Wave Buoy Network (RON), specifically the buoy located offshore of La Spezia (43.9292° N, 9.8278° E). Managed by ISPRA, the buoy provides half-hourly data on significant wave height, wind speed and direction, wave direction, and atmospheric pressure. These measurements were used to characterize the wave field dynamics near the northern Tuscan coast during the storm event.

To contextualize the exceptionality of the event, the historical time series of significant wave height recorded by the buoy from 1989 to 2023 was analyzed. Percentile thresholds (99.0°, 99.5°, 99.9°, and 99.99°) were calculated, and the 3 November 2023 event was compared against these thresholds to determine its statistical rarity.

The synoptic-scale atmospheric conditions were reconstructed using ERA5 reanalysis data, provided by the Copernicus Climate Change Service (C3S). The ERA5 dataset offers hourly global data with a spatial resolution of $0.25° \times 0.25°$. Variables extracted for this analysis include mean sea level pressure (MSL), 10 m wind speed and direction (U10 and Dir), and significant height of wind waves (SHWW).

ERA5 data were processed in Python v3.11 and GIS environments to analyze both atmospheric and marine conditions during the period from 2 to 4 November 2023.

A historical–statistical analysis was conducted to assess the frequency of events comparable to the one on 3 November 2023. ERA5 datasets covering the 1940–2023 period were used. A multivariable threshold was defined based on the observed values during the storm event:

- SHWW $\geq$ 5.01 m;
- U10 $\geq$ 12.95 m/s;
- MSL $\leq$ 985.18 hPa.

An automated search was performed within the dataset to identify all events that simultaneously met the defined threshold conditions. Subsequently, a sensitivity analysis was conducted by progressively relaxing the thresholds with tolerances of 2%, 5%, and 10%, in order to assess the relative frequency and climatological rarity of Storm Ciaran.

Figure 2 summarizes the procedure adopted in this study.

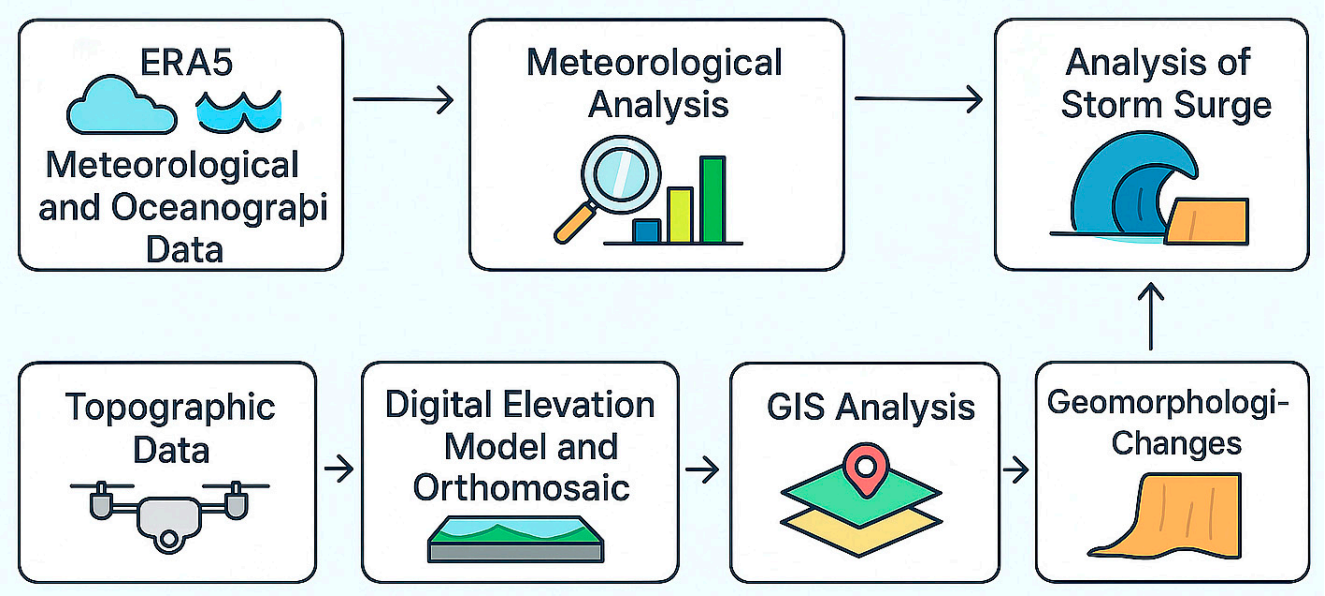


Figure 2. Workflow for analyzing storm surge impacts and coastal morphodynamics.

4. Results

4.1. Description of the Meteorological Event

Figure 3 shows the evolution of the main meteorological and oceanographic parameters observed during Storm Ciaran, which impacted the Pisa coastline on 3 November 2023. The low-pressure system was associated with a sharp drop in atmospheric pressure, reaching a minimum of approximately 984 hPa, and with strong southwesterly winds, ranging between 210° and 250°, with average speeds exceeding 10–15 m/s and a peak gust exceeding 66 km/h. Wind intensity increased rapidly in the hours preceding the peak of the storm surge, contributing to the formation of a well-developed wave field, with significant wave heights exceeding 6 m (with a maximum value of 6.6 m recorded).

The wind and wave roses highlight the dominance of directions between southwest (Libeccio) and south (Mezzogiorno), consistent with the orientation of the coastline in the study area. In particular, wave energy from the SSW direction played a key role in reshaping the beach profile.

Morphological impact assessment was carried out by comparing two high-resolution UAV topographic surveys: one acquired on 19 June 2023 (pre-event conditions), and one acquired immediately after the storm, on 6 November 2023. The June survey was selected as the pre-event reference because no meteomarine events of comparable energy occurred in the intervening period (see Figure 3).

Figure 4 presents the historical time series of significant wave height recorded by the La Spezia buoy from 1989 to the present, along with thresholds corresponding to the 99.0°, 99.5°, 99.9°, and 99.99° percentiles. The 3 November 2023 event exceeded the 99.99th percentile, confirming its exceptional magnitude. In over thirty years of observations, only three other events have matched or exceeded this intensity, further confirming the extraordinary rarity of the storm surge associated with Storm Ciaran.

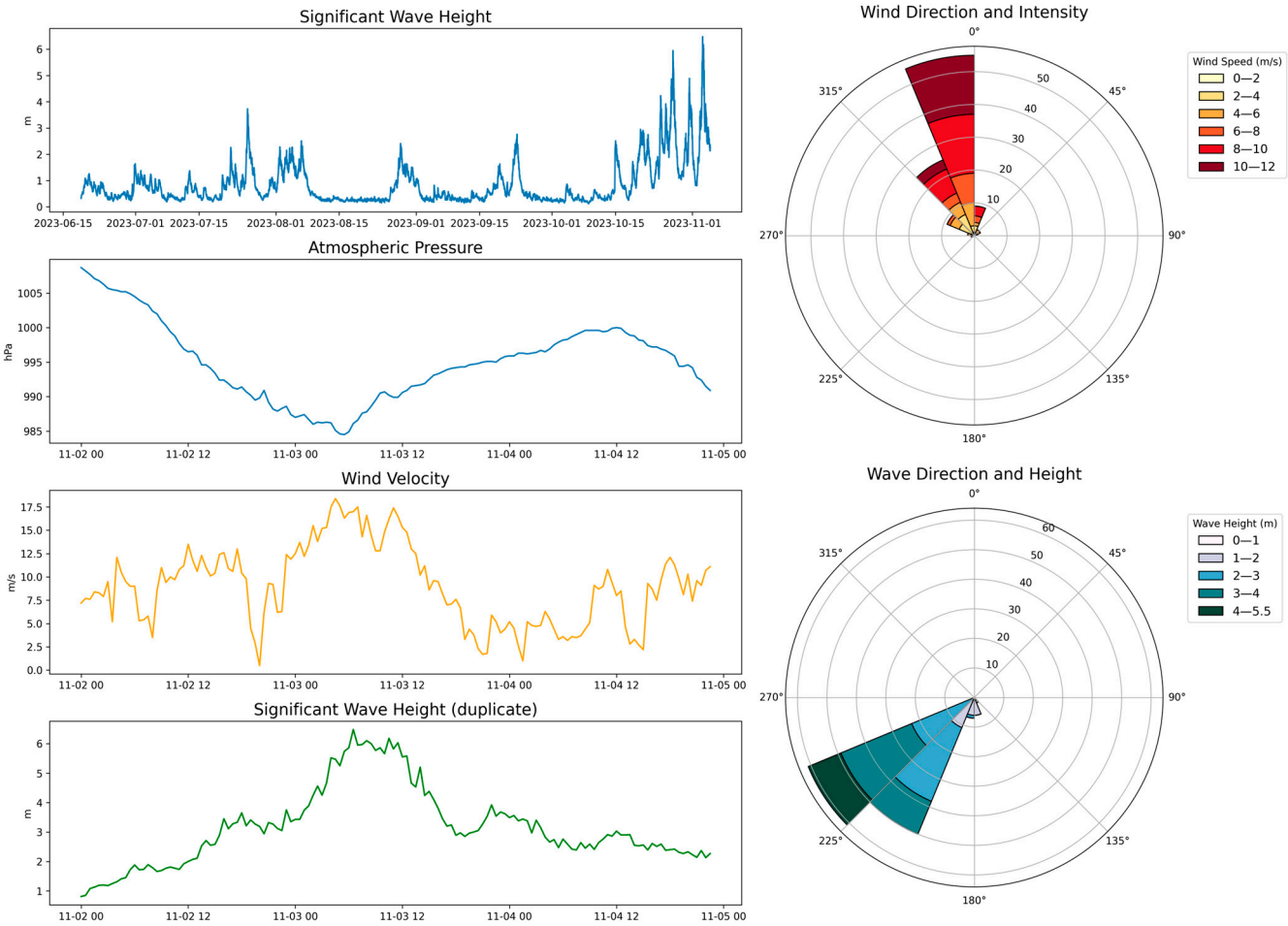


Figure 3. Time series and polar plots of atmospheric and oceanographic parameters during the storm event on 3 November 2023. Panels show wave height, pressure, and wind velocity evolution (**left**), along with wind direction/intensity and wave direction/height distributions (**right**).

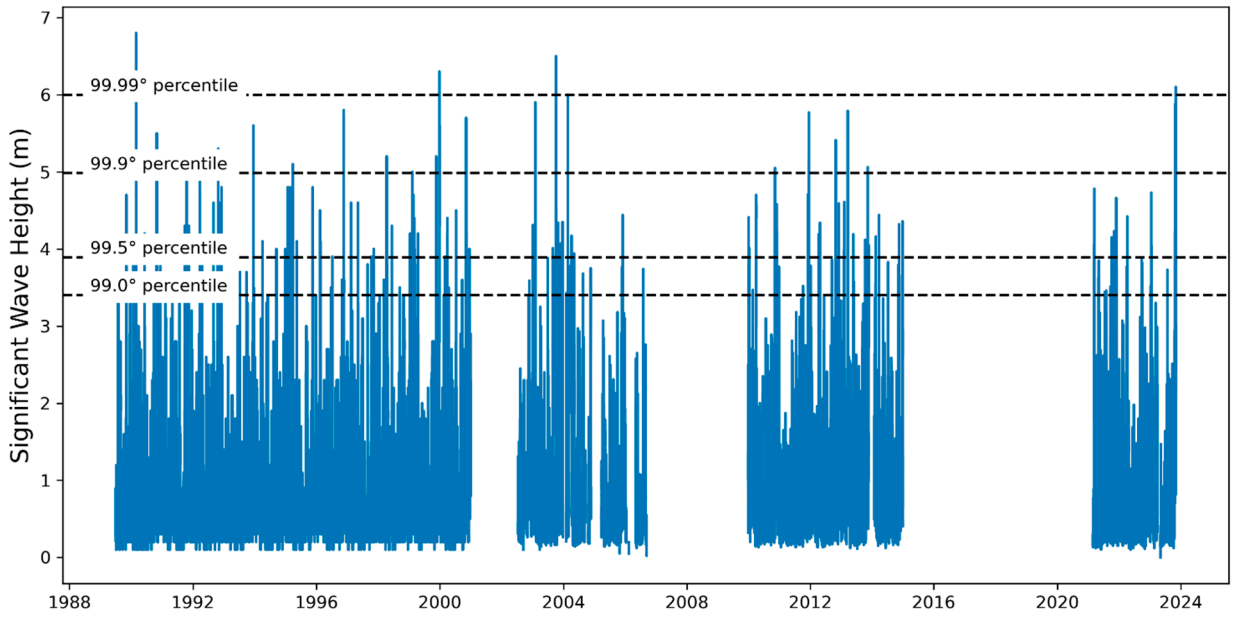


Figure 4. Long-term time series of significant wave height (1990–2024) with thresholds for extreme events marked at the 99.0°, 99.5°, 99.9°, and 99.99° percentiles.

Figure 5 shows an analysis based on ERA5 data, focused on significant wave height (SHWW), 10 m wind speed (U10), and mean sea level pressure (MSL), under conditions similar to those observed during the November 3 event. Panel (a) displays the frequency of events in the ERA5 archive that exactly match the observed parameters (SHWW $\geq$ 5.01 m; U10 $\geq$ 12.95 m/s; MSL $\leq$ 985.18 hPa), revealing that, besides Ciaran, only one similar event occurred in 1977. The subsequent panels show the effect of progressively relaxing the threshold: panel (b), with a 2% margin, identifies 8 events; panel (c), with a 5% tolerance, shows 10 events; and panel (d), with a 10% range, includes 16 events in total. This progressive increase further underscores the rarity of Storm Ciaran, even within a long climatological reanalysis record.

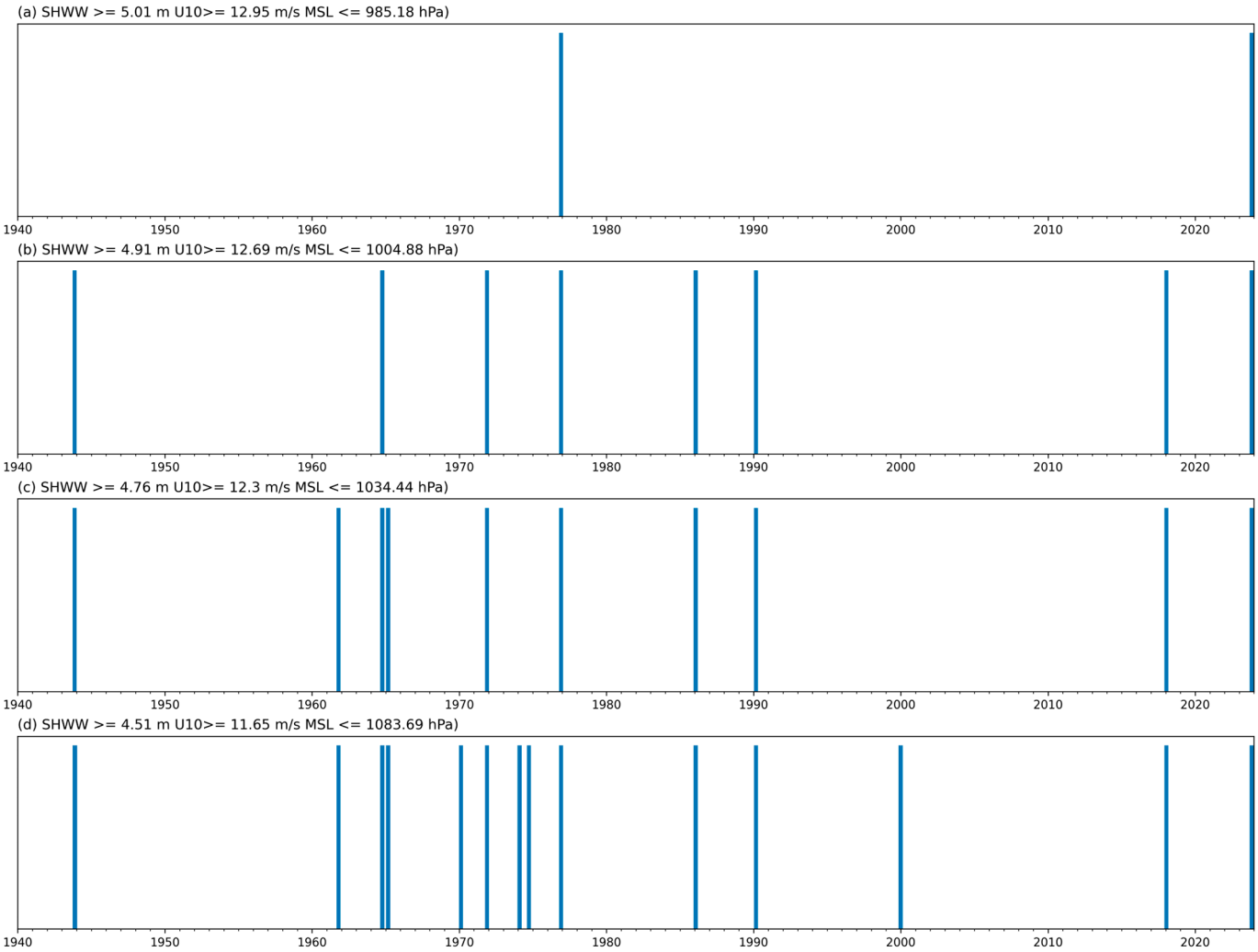


Figure 5. Occurrence of extreme marine storms from 1940 to 2024 under different combined thresholds of significant wave height (SHWW), wind speed at 10 m (U10), and mean sea level pressure (MSL). Panels (**a**–**d**) represent progressively less restrictive conditions.

4.2. Geomorphological Effects

In order to provide a comprehensive understanding of the storm's geomorphological impact, a combination of UAV-derived data and field-based photographic documentation was employed. During the post-event UAV survey conducted on 6 November 2023, a set of field photographs (Figure 6a–c) was taken to visually capture the storm's effects at ground level. These images document severe foredune scarping, vertical exposure of root systems, and vegetation collapse along the dune front, offering direct visual corroboration

of the erosional features identified via UAV analysis. The integration of aerial and on-the-ground evidence enables a richer and more nuanced interpretation of the storm-induced morphological changes along the beach–dune interface.

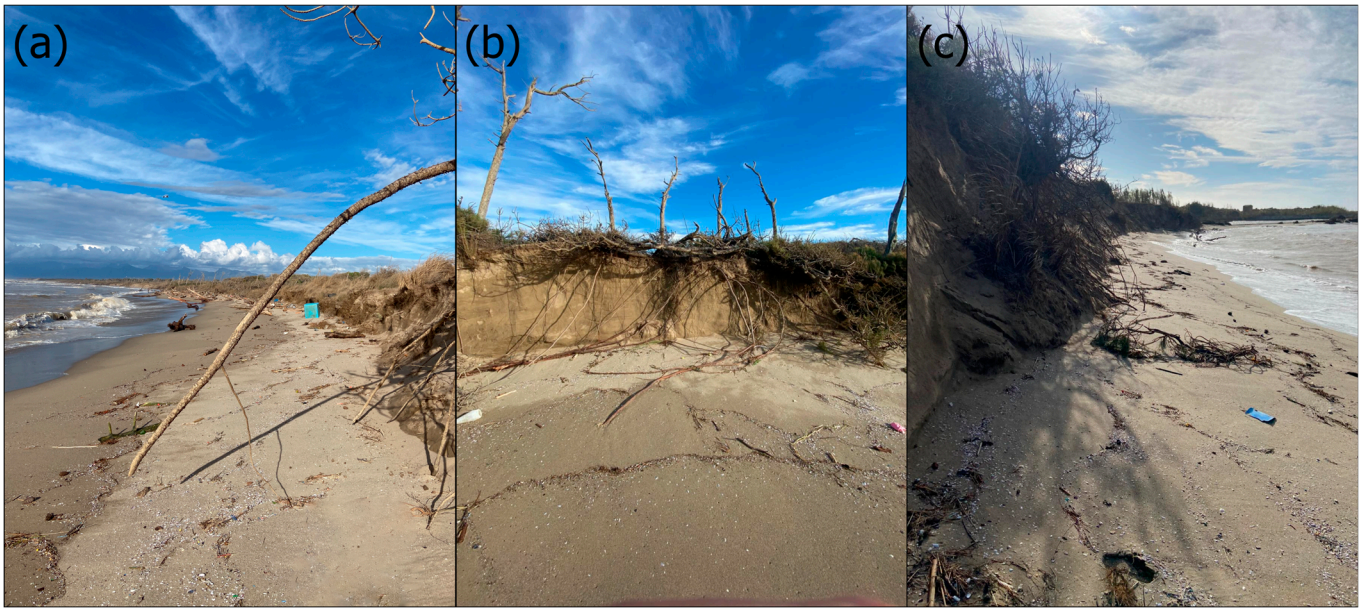


Figure 6. Post-event field documentation: (**a**) post-storm field view looking northward along the study beach, illustrating foredune scarping, broken vegetation, and sediment debris aligned by wave run-up; (**b**) close-up of a vertical dune scarp exposing root systems and collapsed vegetated dune face, indicative of sudden erosion; (**c**) beach narrowing near the river mouth, showing overwash deposits and vegetation damage consistent with storm surge impact.

The photogrammetric processing reports generated with Agisoft Metashape for the UAV surveys conducted in June and November 2023 confirm the high quality of the data acquired for morphological assessment.

The June survey, consisting of 366 images acquired at an average flight altitude of 40.1 m, produced a model with a resolution of 1.96 cm/pixel and a point density of 0.26 pts/cm^2. The mean error on Ground Control Points (GCPs) was 0.43 cm in X, 0.35 cm in Y, and 0.34 cm in Z, with a mean horizontal (XY) error of 0.55 cm and a total spatial error (XYZ) of 0.65 cm, based on seven control points. The four check points showed mean errors of 1.09 cm in X, 1.10 cm in Y, and 1.06 cm in Z, with a mean XY error of 1.55 cm and a total error of 1.88 cm.

The November survey, which covered a larger area, was based on 982 images acquired at a flight altitude of 38.9 m, covering 0.108 km^2 with a resolution of 2.01 cm/pixel. The 15 GCPs recorded mean errors of 0.86 cm in X, 1.05 cm in Y, and 0.35 cm in Z, resulting in an average XY error of 1.36 cm and a total spatial error of 1.40 cm. The 7 check points presented mean errors of 1.56 cm in X, 1.61 cm in Y, and 2.75 cm in Z, with an average XY error of 2.25 cm and a total error of 3.55 cm. The model had a point density of 0.248 pts/cm^2.

The final output included a Digital Elevation Model (DEM) with a resolution of 2.01 cm/pixel for November and 1.96 cm/pixel for June. The generated orthomosaics had a resolution of 2.41 cm/pixel in both cases, corresponding to the pixel size of the onboard camera.

A comparison between the pre- and post-event DEMs, shown in Figure 7, illustrates the morphological configuration of the coastal system before and after the storm. The June 2023 model (panel A) reveals a continuous and gently sloping beach backed by a

well-preserved dune front, while the November 2023 model (panel B) shows significant morphological alterations. In particular, the loss of dune volume and the formation of steep scarp faces are visible in the central and southern sectors.

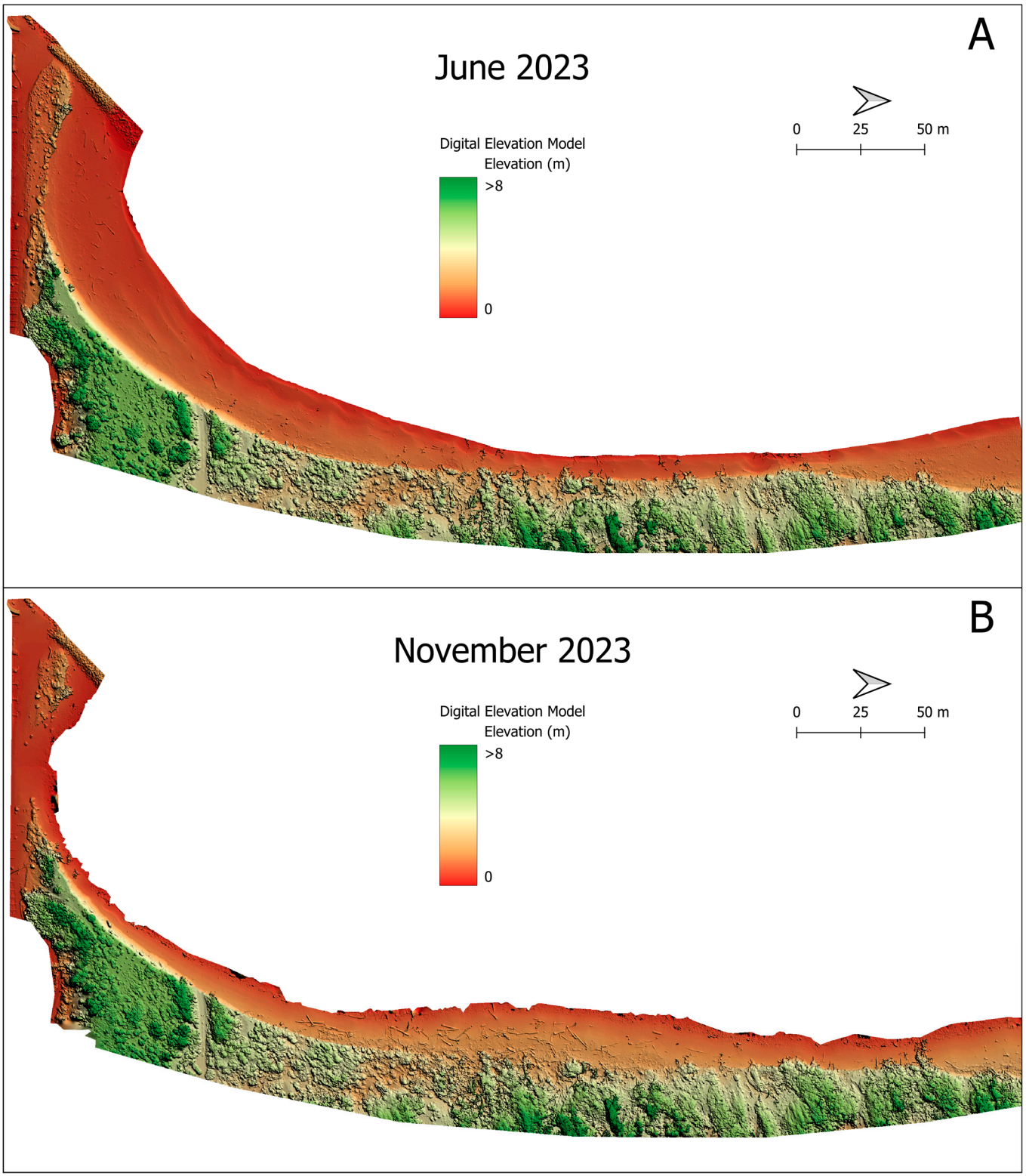


Figure 7. Digital Elevation Models (DEMs) of the study area derived from UAV surveys conducted in June 2023 (panel **A**) and November 2023 (panel **B**), before and after the storm event. Elevation is expressed in meters and visualized using a hillshade and hypsometric color scale ranging from 0 m (red) to >8 m (green).

Figure 8 illustrates the comparison between the pre-event (June 2023) and post-event (November 2023) surveys, highlighting shoreline displacement and elevation change of the emerged beach. Colored lines indicate the shoreline position in the two surveys, while the difference map shows erosional areas in red (lowering) and accretion areas in green (raising). Regarding the shoreline, an average advance of 6.64 m (maximum of 12.93 m) was observed, alongside an average retreat of −12.68 m and a maximum of −30.10 m. Overall, the mean displacement of the shoreline front was −5.45 m, indicating a net landward retreat of the coastal system. The areas affected by morphological changes covered 13,066.49 m^2 of erosion and 10,664.03 m^2 of accretion, for a total modified area of 23,730.52 m^2. In volumetric terms, the eroded areas accounted for a total sediment loss of 6632.81 m^3, while the accretion areas gained 4840.48 m^3, resulting in a net sediment budget of −1792.33 m^3.

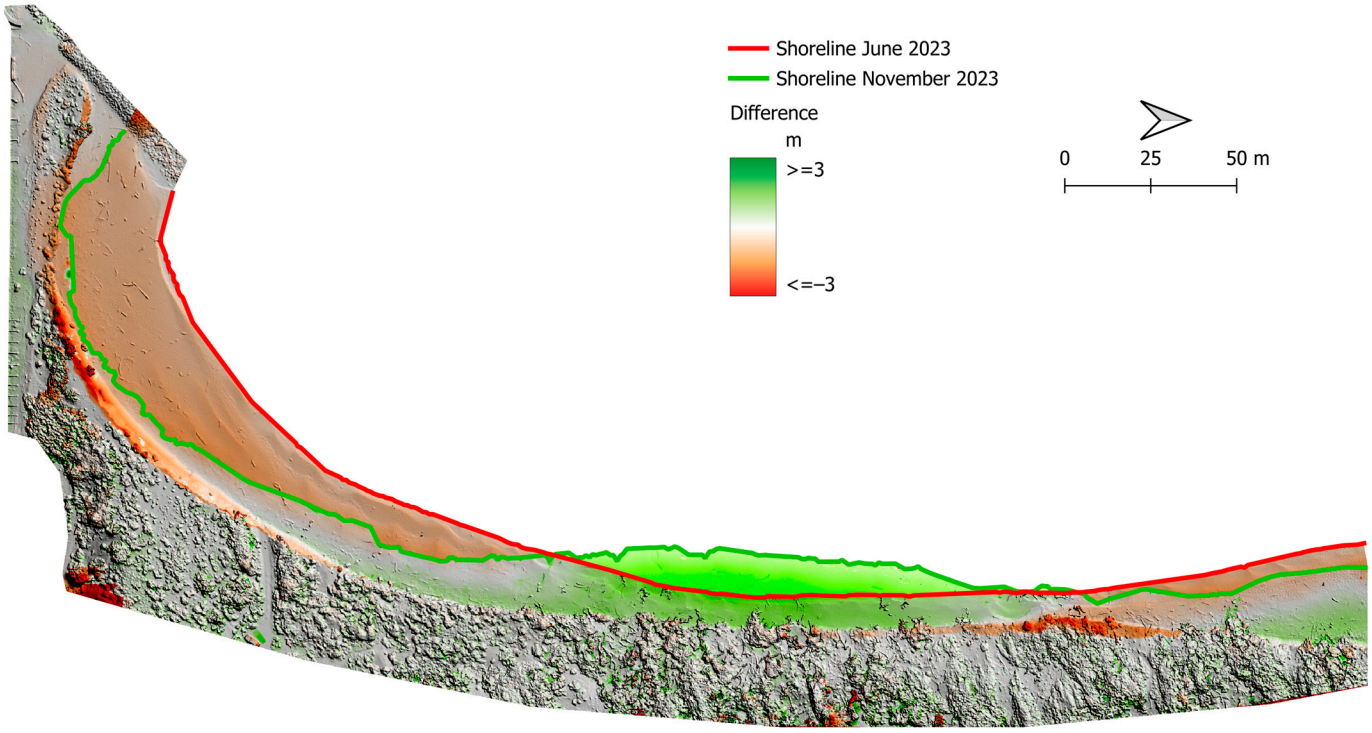


Figure 8. Shoreline change between June and November 2023 overlaid on a topographic difference map. Green and red zones indicate areas of accretion and erosion, respectively.

Figure 9 shows the distribution of slope variations along cross-shore transects spaced approximately every 5 m. The transects are colored according to the change in beach slope (in degrees) between the November and June surveys. The data clearly show two distinct patterns: in erosional areas, the slope increased, indicating a steepening of the beach face, while in accretion areas the slope decreased, forming a gentler profile.

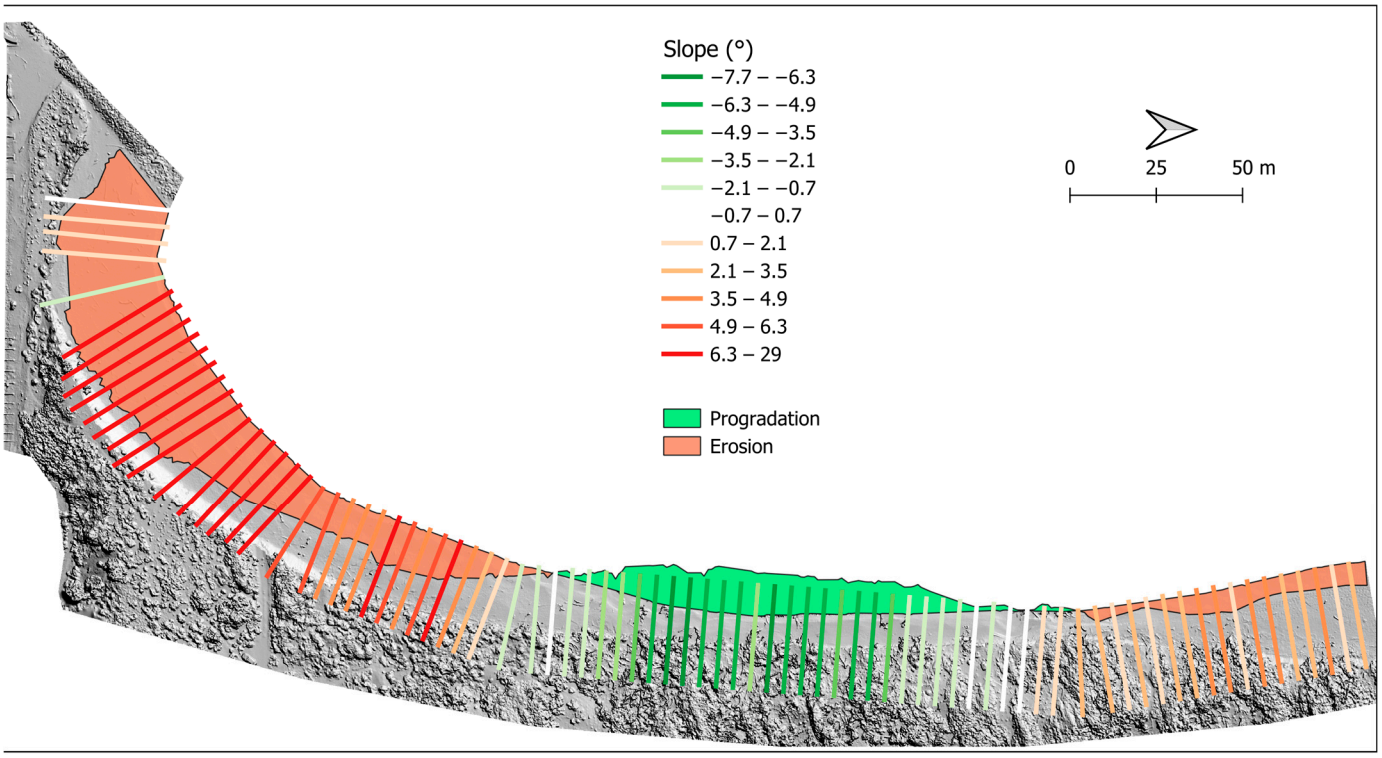


Figure 9. Variation in beach slope between June and November 2023 along cross-shore transects. Colors indicate the change in slope (in degrees), with red tones representing steepening (erosion-dominated) and green tones indicating flattening (progradation-dominated).

To complement the DEM comparison and shoreline analysis, Figure 10 further illustrates the morphological evolution of the beach–dune system through a series of 12 cross-shore elevation profiles extracted from the UAV-derived models. These transects, distributed approximately every 5 m along the study area, provide detailed insights into localized topographic changes. Notably, several profiles (e.g., Transects 13 and 67) clearly show a landward shift of the dune toe, indicating significant erosion at the base of the foredune. This shift is frequently accompanied by an increase in profile steepness, as observed in Transects 25 and 73, where the beach face has become markedly steeper between June and November 2023. In contrast, other sectors exhibit signs of sediment accumulation, such as in Transects 31, 37, 43, and 49, where the beach appears to have prograded seaward. However, this accretion is coupled with a noticeable lowering of the dune crest, suggesting structural weakening or partial collapse of the dune front. Overall, the profiles highlight a complex spatial pattern of erosion and deposition, underscoring the dynamic response of the beach–dune system to storm-induced forcing.

Figure 11 presents the dune toe position analysis, derived from Sky-View Factor (SVF) images generated from the DEMs. Green and red lines indicate the dune toe positions detected in June and November, respectively. Quantitative analysis shows that, even in areas classified as accreting based on shoreline and volumetric data, a setback of the dune toe occurred, indicating that erosional processes also affected those zones. The maximum dune toe advance was 3.36 m, while the average retreat was −1.93 m, with a maximum of nearly −7 m. The average total displacement was −1.6 m, with 88% of the analyzed sector showing retreat and only 12% showing advance.

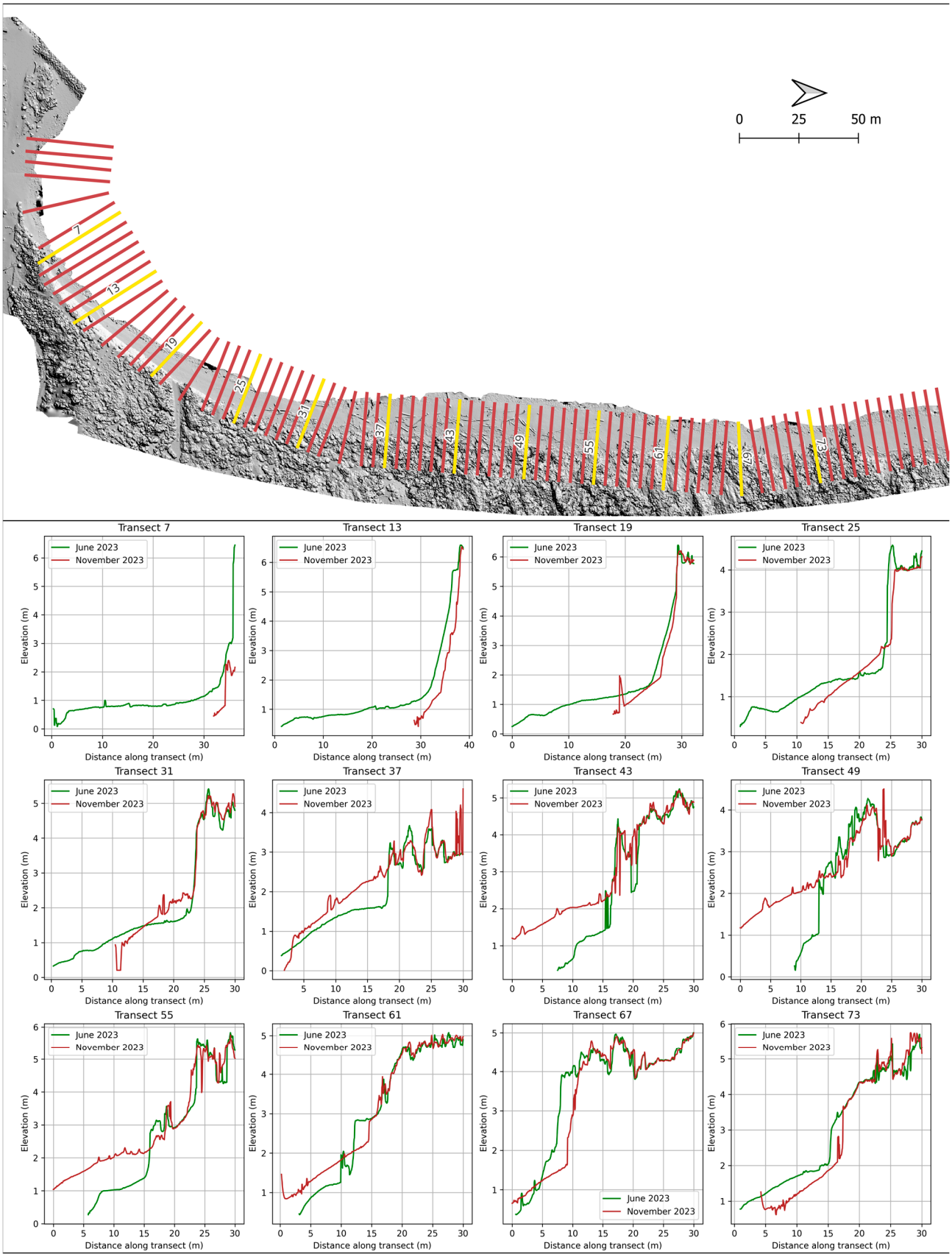


Figure 10. (Top): Hillshade view (November 2023) of the monitored coastal sector with transects (red lines) used to extract elevation profiles from June 2023 and November 2023 digital surface models. Selected transects (yellow labels) are shown in the plots below. (**Bottom**): Elevation profiles along 12 representative transects (7 to 73), comparing surface morphology between June 2023 (green line) and November 2023 (red line).

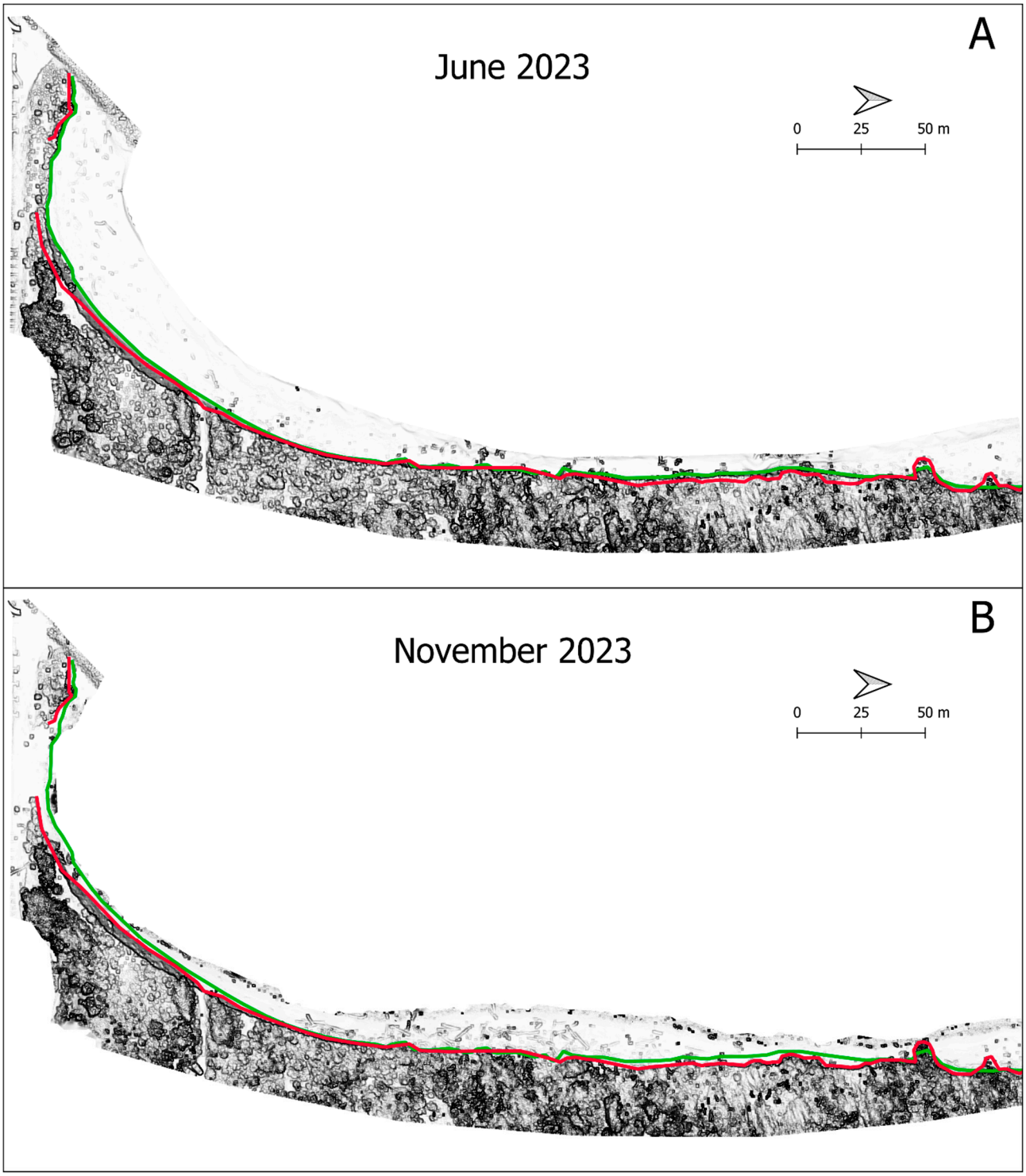


Figure 11. Position of the dune toe in June (green) and November (red) 2023 overlaid on sky-view factor images. Panel (**A**) shows the June survey, while panel (**B**) displays the November survey.

5. Discussion

The event of 3 November 2023 offers a key opportunity to reflect on the growing vulnerability of Mediterranean coasts in the context of intensifying meteomarine forcing and increasing uncertainty related to the frequency and intensity of extreme events [1,9]. Their episodic nature and the lack of high-resolution, systematic time series make it difficult to identify clear trends and the synoptic conditions that generate them, as highlighted by studies emphasizing the complexity of meteorological variability in the Mediterranean and

the need for more continuous, high-quality data for the analysis of extreme events [60]. In this context, every study that documents such phenomena in detail contributes fundamentally to understanding coastal processes and defining coherent adaptation strategies.

It is important to acknowledge that the five-month interval between the two UAV surveys may allow for the influence of background low-energy processes, such as daily tidal action, minor wave-induced sediment reworking, or undetected human activity. Although no significant meteomarine events occurred in the intervening period, as confirmed by buoy data, these cumulative minor processes may have contributed to subtle morphological modifications. However, the magnitude and spatial extent of the changes observed, especially the marked shoreline retreat and dune toe regression, are orders of magnitude greater than those typically associated with low-intensity background dynamics. Therefore, while a degree of uncertainty remains, the dominant geomorphological signal can be confidently attributed to the impact of the 3 November 2023 event.

There is a clear need for integrated, continuous monitoring based not only on shoreline position but also on volumetric and altimetric morphological parameters. This study has shown that dune toe retreat can occur even in sectors apparently advancing when only the shoreline position is considered, demonstrating that shoreline analysis alone is often insufficient to fully represent coastal dynamics or the actual impact of extreme events. The slope variations observed along shore-perpendicular transects reflect typical high-energy storm morphodynamics. In particular, erosion tends to lower the coastal profile, often accompanied by a steepening of the slope and the formation of a more vertical beach face [61]. Conversely, progradational areas show a decrease in slope, forming gentler profiles. However, even during high-energy events such as the one analyzed in this study, temporary sediment deposition can occur, leading to flatter beach profiles [62]. In addition to widespread erosion, the analysis also reveals the presence of well-defined depositional zones, particularly in the northern and central sectors of the study area (Figure 8). These zones, despite the overall negative sediment budget, experienced measurable sediment accumulation, contributing to a local flattening of the beach profile. Their occurrence suggests that storm events can redistribute sediment unevenly, creating small-scale accumulation areas that may temporarily mitigate the erosional signal. This highlights the need to consider both erosional and accretional dynamics when assessing the geomorphological impact of extreme events.

Such erosion and deposition processes are not always uniform along the coast, but can occur in a localized manner, generating morphological hotspots that represent areas of heightened vulnerability or sediment recovery [63]. The integration of high-resolution monitoring techniques, such as those based on Digital Elevation Models (DEMs) from UAV photogrammetric surveys, is therefore essential for capturing coastal morphological responses to extreme events. These tools allow for precise detection of both localized and transient topographic variations, greatly improving our understanding of beach erosion, progradation, and reshaping processes. When acquired regularly over time, such data represent a fundamental resource for the development of more informed and responsive coastal management strategies.

In the study area, four nourishment interventions were carried out between 2010 and 2013, for a total volume of approximately 3500 m^3 of sediment, distributed along the coast to mitigate erosion [8]. The extreme weather event associated with Storm Ciaran generated a net sediment budget deficit of about 1800 m^3, corresponding to over 50% of the total volume added through these soft interventions. Furthermore, the average shoreline retreat rate in this stretch of coast over the last 40 years is approximately 5–6 m per year [21], yet the impact of a single intense storm such as Ciaran shows a comparable magnitude. In fact, the event caused an average shoreline retreat exceeding 5 m, with localized peaks up to 30 m,

values typically recorded over the course of a full year. A similar trend was observed in the dune toe position, which showed an average retreat of over 2 m, with maximum values close to 7 m.

These results highlight that long-term erosion rates may derive not only from continuous, diffuse retreat processes but also from the cumulative effect of sporadic, high-intensity extreme events. Understanding the relative contribution of these components is crucial for guiding effective coastal planning, both in terms of the frequency and scale of nourishment operations and the design and placement of hard protection structures.

Although a small difference in sea level is present between the two UAV surveys (approximately 40 cm, based on IOC tide gauge data from the Livorno station), the shoreline position in this study was not determined by the instantaneous waterline, but by a slope-break detection method applied to high-resolution DEMs. Moreover, this study does not rely solely on shoreline retreat, but places strong emphasis on dune erosion and scarping processes, which cannot be attributed to tidal fluctuations. This confirms that the use of a single geomorphological indicator is insufficient for a comprehensive analysis of coastal change. A multi-parameter approach, including volumetric loss, slope changes, and dune toe regression, provides a more robust and meaningful interpretation of storm-induced morphological dynamics.

The morphodynamic responses observed in this study, including shoreline retreat, dune toe regression, and sediment deficits following a single extreme storm, are consistent with recent findings from other Mediterranean coastal systems characterized by microtidal conditions and limited sediment supply. For example, on a natural beach in southwestern Sardinia, the authors of [64] documented significant morphological changes, including shoreline retreat and the formation of Posidonia oceanica beach-cast deposits, occurring over a very short timescale following high-energy storm events on a natural microtidal beach in southwestern Sardinia. In Menorca Island, in the western Mediterranean, the authors of [65] used numerical simulations to demonstrate how the presence of a wide berm can reduce the retreat of the shoreline under storm and sea level rise scenarios. Along the Adriatic coast of southern Italy, the authors of [66] observed the retreat of the dune toe, the formation of washover channels, and sediment redistribution on the beach–dune barrier of Cesine Lagoon in response to storm-driven wind and wave conditions. These examples support the idea that the processes described in our study are not isolated, but instead reflect regional patterns of vulnerability and response across Mediterranean sandy coasts.

In the specific case studied, the defense structures built and maintained since 2011 proved to be ineffective: the areas most severely impacted during the storm were in fact located in the immediate vicinity of these structures, suggesting potential energy concentration effects or negative alteration of natural morphodynamics. This ineffectiveness may be related to several well-known physical mechanisms. Hard coastal structures can reflect incoming wave energy, increasing turbulence and promoting scouring at their base [6,11,67]. They often disrupt longshore sediment transport, causing sediment accumulation updrift and deficit downdrift, which may enhance erosion in adjacent unprotected sectors [68]. In addition, the presence of groins or breakwaters can lead to wave refraction and diffraction, concentrating energy at structure edges or around gaps, further exacerbating localized erosion [69]. These effects can be especially pronounced under high-energy storm conditions, as observed during the impact of the event studied.

During the storm, the collapse of the remaining dune section at the southern edge of the study area (Figure 12), which previously ensured the separation between marine waters and the inland drainage network, resulted in direct contact between the sea and the reclamation system. This event caused malfunctions and delays in the drainage of stormwater, along

with significant ecological impacts. These findings confirm that the integrity of the dune is not only a geomorphological element, but also a natural infrastructure essential for the hydrological and environmental stability of the coastal plain.

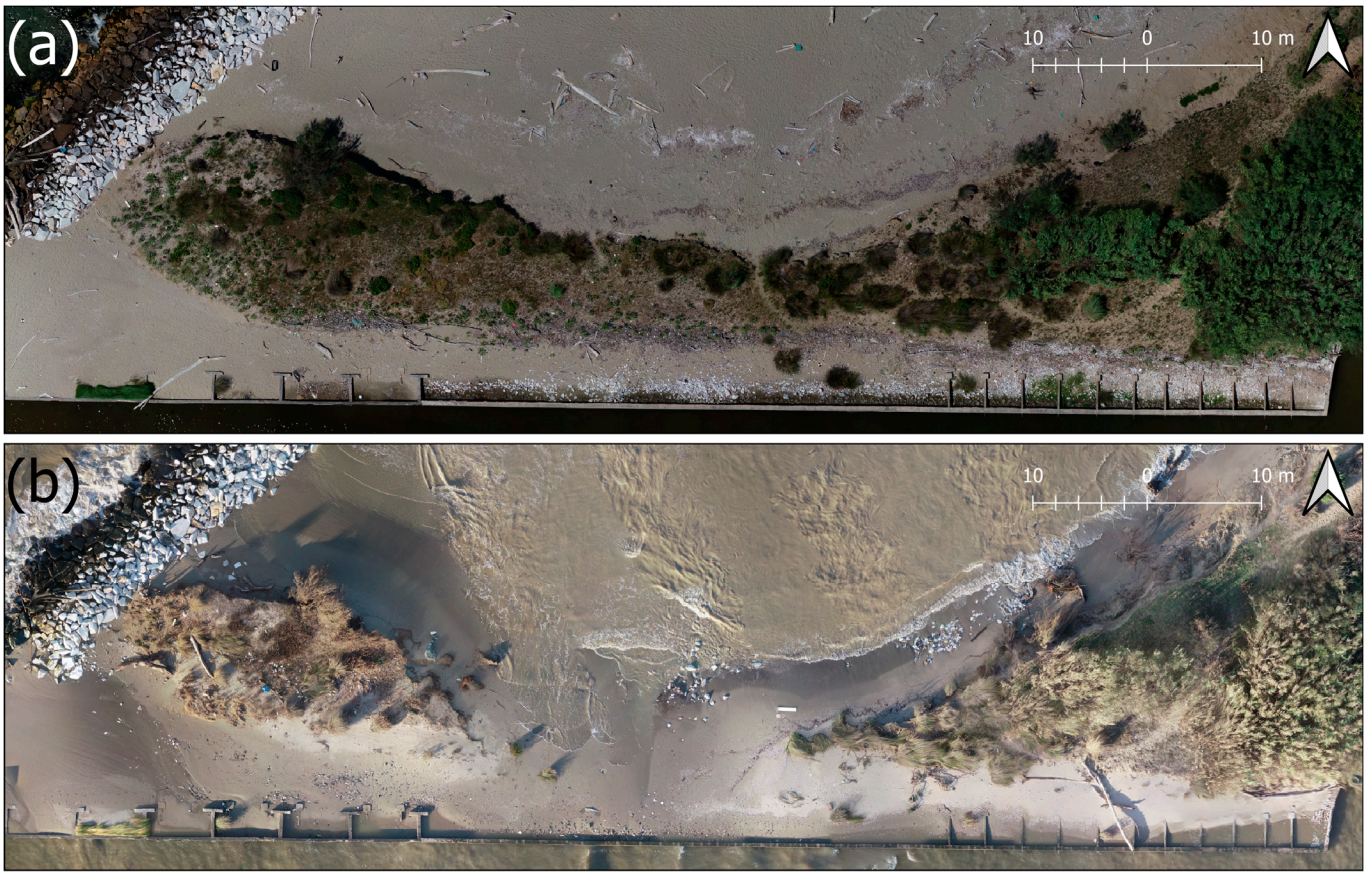


Figure 12. Orthomosaics acquired in June 2023 (**a**) and November 2023 (**b**) showing the dismantling of the dune system at the southern end of the study area. The breach led to direct contact between seawater and the drainage canal of the reclamation system, compromising the separation between marine and inland waters.

Given the low effectiveness of the groin built to protect this sector, an inefficacy also seen in other hard defense systems along the littoral cell, such as the barriers at Gombo and Marina di Pisa or the groins in the Lame della Gelosia area, it is essential to incorporate climate change variables into coastal defense planning. These include the increased intensity of storm events and rising mean sea level.

At the same time, it is necessary to promote flexible and nature-based adaptation strategies, such as soft nourishment, managed retreat, and dune system restoration. These approaches offer more sustainable and resilient alternatives to hard defenses, which should remain a last resort, used only when morphological and socio-economic conditions leave no viable alternatives [70].

The quantification of morphological variations (dune toe retreat, shoreline dynamics, beach slope changes, and sediment volume loss) induced by a single storm event highlights the importance of understanding the impact of extreme events on the coast and the need to invest in the modernization of morphodynamic evolution models, including the integration of advanced numerical codes and artificial intelligence for predicting sediment transport and deposition.

To address these vulnerabilities, a combination of structural and non-structural coastal protection measures should be considered. Structural interventions may include groins,

submerged breakwaters, revetments, and seawalls, though their long-term effectiveness in dynamic sandy environments remains debated. On the other hand, non-structural solutions such as soft nourishment, managed retreat, dune restoration, and early warning systems offer more flexible and adaptive responses, especially in protected natural areas. These approaches, when supported by high-resolution monitoring and climate-informed planning, can enhance the resilience of coastal systems to future storm impacts.

6. Conclusions

The storm surge of 3 November 2023 represents an emblematic case of the effects that extreme meteomarine events can have on low-lying and sandy Mediterranean coasts. The impact observed in the southern sector of the study area revealed an average shoreline retreat exceeding 5 m, with local peaks up to 30 m, and dune toe regression reaching 7 m at the most exposed locations. Overall, the event resulted in a net sediment deficit of approximately 1800 m^3, equivalent to more than 50% of the total volume added during soft nourishment interventions carried out in the previous decade.

These data emphasize how the impact of a single storm event can match, in both intensity and magnitude, the average annual erosion rate, highlighting the need to reinterpret long-term retreat trends in relation to the frequency and severity of extreme events. The episodic nature of such phenomena, combined with the lack of high-resolution temporal and spatial datasets, poses a substantial challenge for coastal management and defense planning.

The integration of high-resolution monitoring techniques, based on UAV-SfM surveys and multi-parametric morphological analyses, enabled the detailed quantification of the storm's effects on several geomorphological components, including shoreline retreat, dune toe regression, and both volumetric and altimetric changes of the beach profile. This integrated approach allowed for a more comprehensive assessment of the event's impact, underlining the importance of using multiple morphological indicators to understand erosion dynamics and the overall health of the coastal system.

The event also exposed the limitations of existing hard defense structures, which proved largely ineffective in mitigating damage, as the most severely impacted areas were located precisely near these structures. This underscores the urgent need to revisit planning strategies in light of increasing uncertainty imposed by climate change, explicitly incorporating the expected intensification of storm events, sea level rise, and the increasing instability of coastal systems.

Although this study focuses on a specific case, the results contribute to a broader national framework where similar phenomena are increasingly frequent and well documented, driven by an increasingly fragile environmental context. Understanding how often such intense events may occur, what local mechanisms drive their impact, and which strategies are most effective in response represents a critical priority for integrated coastal zone management in Italy.

Future work should focus on integrating high-resolution time series, employing advanced numerical models, potentially supported by artificial intelligence techniques, and developing continuous monitoring systems that combine UAV data, fixed sensors, and satellite remote sensing. Only through such an integrated approach will it be possible to develop more targeted, resilient, and sustainable response strategies to meet the challenges posed by climate change along the coastlines.

Funding: This research was funded by the **Autorità di Bacino Distrettuale dell'Appennino Settentrionale**—*Misure di prevenzione tese a supportare ed ottimizzare la pianificazione di gestione, la programmazione e realizzazione degli interventi di cui al PGRA* (F54J16000020001).

Data Availability Statement: The original contributions presented in this study are included in the article. Further inquiries can be directed to the corresponding author.

Conflicts of Interest: The authors declare no conflict of interest.

References

1. Zhang, K.; Douglas, B.C.; Leatherman, S.P. Global Warming and Coastal Erosion. *Clim. Change* **2004**, *64*, 41–58. [CrossRef]
2. Giorgi, F. Climate Change Hot-Spots. *Geophys. Res. Lett.* **2006**, *33*, L08707. [CrossRef]
3. Tuel, A.; Eltahir, E.A.B. Why Is the Mediterranean a Climate Change Hot Spot? *J. Clim.* **2020**, *33*, 5829–5843. [CrossRef]
4. Lazoglou, G.; Papadopoulos-Zachos, A.; Georgiades, P.; Zittis, G.; Velikou, K.; Manios, E.M.; Anagnostopoulou, C. Identification of Climate Change Hotspots in the Mediterranean. *Sci. Rep.* **2024**, *14*, 29817. [CrossRef] [PubMed]
5. Besset, M.; Anthony, E.J.; Bouchette, F. Multi-Decadal Variations in Delta Shorelines and Their Relationship to River Sediment Supply: An Assessment and Review. *Earth Sci. Rev.* **2019**, *193*, 199–219. [CrossRef]
6. Pranzini, E.; Anfuso, G.; Cinelli, I.; Piccardi, M.; Vitale, G. Shore Protection Structures Increase and Evolution on the Northern Tuscany Coast (Italy): Influence of Tourism Industry. *Water* **2018**, *10*, 1647. [CrossRef]
7. Rangel-Buitrago, N.; Williams, A.T.; Anfuso, G. Hard Protection Structures as a Principal Coastal Erosion Management Strategy along the Caribbean Coast of Colombia. A Chronicle of Pitfalls. *Ocean. Coast Manag.* **2018**, *156*, 58–75. [CrossRef]
8. Bertoni, D.; Bini, M.; Luppichini, M.; Cipriani, L.E.; Carli, A.; Sarti, G. Anthropogenic Impact on Beach Heterogeneity within a Littoral Cell (Northern Tuscany, Italy). *J. Mar. Sci. Eng.* **2021**, *9*, 1–22. [CrossRef]
9. Toimil, A.; Camus, P.; Losada, I.J.; Le Cozannet, G.; Nicholls, R.J.; Idier, D.; Maspataud, A. Climate Change-Driven Coastal Erosion Modelling in Temperate Sandy Beaches: Methods and Uncertainty Treatment. *Earth Sci. Rev.* **2020**, *202*, 103110. [CrossRef]
10. Anthony, E.J.; Marriner, N.; Morhange, C. Human Influence and the Changing Geomorphology of Mediterranean Deltas and Coasts over the Last 6000years: From Progradation to Destruction Phase? *Earth Sci. Rev.* **2014**, *139*, 336–361. [CrossRef]
11. Williams, A.T.; Rangel-Buitrago, N.; Pranzini, E.; Anfuso, G. The Management of Coastal Erosion. *Ocean. Coast Manag.* **2018**, *156*, 4–20. [CrossRef]
12. Calvin, K.; Dasgupta, D.; Krinner, G.; Mukherji, A.; Thorne, P.W.; Trisos, C.; Romero, J.; Aldunce, P.; Barrett, K.; Blanco, G.; et al. *IPCC, 2023: Climate Change 2023: Synthesis Report. Contribution of Working Groups I, II and III to the Sixth Assessment Report of the Intergovernmental Panel on Climate Change*; Core Writing Team, Lee, H., Romero, J., Eds.; IPCC: Geneva, Switzerland, 2023.
13. Aiello, A.; Canora, F.; Pasquariello, G.; Spilotro, G. Shoreline Variations and Coastal Dynamics: A Space–Time Data Analysis of the Jonian Littoral, Italy. *Estuar. Coast. Shelf Sci.* **2013**, *129*, 124–135. [CrossRef]
14. Manca, E.; Pascucci, V.; Deluca, M.; Cossu, A.; Andreucci, S. Shoreline Evolution Related to Coastal Development of a Managed Beach in Alghero, Sardinia, Italy. *Ocean. Coast Manag.* **2013**, *85*, 65–76. [CrossRef]
15. Alberico, I.; Amato, V.; Aucelli, P.; Paola, G.; Pappone, G.; Rosskopf, C. Historical and Recent Changes of the Sele River Coastal Plain (Southern Italy): Natural Variations and Human Pressures. *Rend. Lincei* **2012**, *23*, 3–12. [CrossRef]
16. Rosskopf, C.M.; Di Paola, G.; Atkinson, D.E.; Rodríguez, G.; Walker, I.J. Recent Shoreline Evolution and Beach Erosion along the Central Adriatic Coast of Italy: The Case of Molise Region. *J. Coast. Conserv.* **2018**, *22*, 879–895. [CrossRef]
17. Borzì, L.; Anfuso, G.; Manno, G.; Distefano, S.; Urso, S.; Chiarella, D.; Di Stefano, A. Shoreline Evolution and Environmental Changes at the NW Area of the Gulf of Gela (Sicily, Italy). *Land* **2021**, *10*, 1034. [CrossRef]
18. Laksono, F.A.T.; Borzì, L.; Distefano, S.; Di Stefano, A.; Kovács, J. Shoreline Prediction Modelling as a Base Tool for Coastal Management: The Catania Plain Case Study (Italy). *J. Mar. Sci. Eng.* **2022**, *10*, 1988. [CrossRef]
19. Lapietra, I.; Lisco, S.; Mastronuzzi, G.; Milli, S.; Pierri, C.; Sabatier, F.; Scardino, G.; Moretti, M. Morpho-Sedimentary Dynamics of Torre Guaceto Beach (Southern Adriatic Sea, Italy). *J. Earth Syst. Sci.* **2022**, *131*, 64. [CrossRef]
20. Celata, F.; Gioia, E. Resist or Retreat? Beach Erosion and the Climate Crisis in Italy: Scenarios, Impacts and Challenges. *Appl. Geogr.* **2024**, *169*, 103335. [CrossRef]
21. Luppichini, M.; Bini, M. 40-Year Shoreline Evolution in Italy: Critical Challenges in River Delta Regions. *Estuar. Coast. Shelf Sci.* **2025**, *315*, 109166. [CrossRef]
22. Billi, P.; Rinaldi, M. Human Impact on Sediment Yield and Channel Dynamics in the Arno River (Central Italy). *IAHS Publ.-Ser. Proc. Rep.-Intern Assoc Hydrol. Sci.* **1997**, *245*, 301.
23. Rinaldi, M. Recent Channel Adjustments in Alluvial Rivers of Tuscany, Central Italy. *Earth Surf. Process. Landf. J. Br. Geomorphol. Res. Group* **2003**, *28*, 587–608. [CrossRef]
24. Surian, N.; Rinaldi, M. Channel Adjustments in Response to Human Alteration of Sediment Fluxes: Examples from Italian Rivers. *IAHS Publ.* **2004**, *288*, 276–282.
25. Surian, N.; Rinaldi, M.; Pellegrini, L.; Audisio, C.; Maraga, F.; Teruggi, L.; Turitto, O.; Ziliani, L. Channel Adjustments in Northern and Central Italy over the Last 200 Years. *Spec. Pap. Geol. Soc. Am.* **2009**, *451*, 83–95. [CrossRef]

26. Bini, M.; Casarosa, N.; Luppichini, M. Exploring the Relationship between River Discharge and Coastal Erosion: An Integrated Approach Applied to the Pisa Coastal Plain (Italy). *Remote Sens.* **2021**, *13*, 226. [CrossRef]
27. Luppichini, M.; Lazzarotti, M.; Bini, M. Climate Change as Main Driver of Centennial Decline in River Sediment Transport across the Mediterranean Region. *J. Hydrol.* **2024**, *636*, 131266. [CrossRef]
28. Cipriani, L.E.; Ferri, S.; Iannotta, P.; Paolieri, F.; Pranzini, E. Morfologia e Dinamica Dei Sedimenti Del Litorale Della Toscana Settentrionale. *Studi Costieri* **2001**, *4*, 119–156.
29. Bini, M.; Casarosa, N.; Ribolini, A. L'evoluzione Diacronica Della Linea Di Riva Del Litorale Pisano (1938-2004) Sulla Base Del Confront Di Immagini Aeree Georeferenziate. *Atti Della Soc. Toscana Di Sci. Nat. Mem. Ser. A* **2008**, *113*, 1–12.
30. Anfuso, G.; Pranzini, E.; Vitale, G. An Integrated Approach to Coastal Erosion Problems in Northern Tuscany (Italy): Littoral Morphological Evolution and Cell Distribution. *Geomorphology* **2011**, *129*, 204–214. [CrossRef]
31. Gonçalves, J.A.; Henriques, R. UAV Photogrammetry for Topographic Monitoring of Coastal Areas. *ISPRS J. Photogramm. Remote Sens.* **2015**, *104*, 101–111. [CrossRef]
32. Turner, I.L.; Harley, M.D.; Drummond, C.D. UAVs for Coastal Surveying. *Coast. Eng.* **2016**, *114*, 19–24. [CrossRef]
33. Taddia, Y.; Corbau, C.; Zambello, E.; Pellegrinelli, A. UAVs for Structure-From-Motion Coastal Monitoring: A Case Study to Assess the Evolution of Embryo Dunes over a Two-Year Time Frame in the Po River Delta, Italy. *Sensors* **2019**, *19*, 1717. [CrossRef]
34. Scicchitano, G.; Scardino, G.; Tarascio, S.; Monaco, C.; Barracane, G.; Locuratolo, G.; Milella, M.; Piscitelli, A.; Mazza, G.; Mastronuzzi, G. The First Video Witness of Coastal Boulder Displacements Recorded during the Impact of Medicane "Zorbas" on Southeastern Sicily. *Water* **2020**, *12*, 1497. [CrossRef]
35. Rizzo, A.; De Giosa, F.; Donadio, C.; Scardino, G.; Scicchitano, G.; Terracciano, S.; Mastronuzzi, G. Morpho-Bathymetric Acoustic Surveys as a Tool for Mapping Traces of Anthropogenic Activities on the Seafloor: The Case Study of the Taranto Area, Southern Italy. *Mar. Pollut. Bull.* **2022**, *185*, 114314. [CrossRef]
36. Novais, J.; Vieira, A.; Bento-Gonçalves, A.; Silva, S.; Folharini, S.; Marques, T. The Use of UAVs for Morphological Coastal Change Monitoring—A Bibliometric Analysis. *Drones* **2023**, *7*, 629. [CrossRef]
37. Sabato, G.; Scardino, G.; Kushabaha, A.; Casagrande, G.; Chirivì, M.; Fontolan, G.; Fracaros, S.; Luparelli, A.; Spadotto, S.; Scicchitano, G. Remote Measurement of Tide and Surge Using a Deep Learning System with Surveillance Camera Images. *Water* **2024**, *16*, 1365. [CrossRef]
38. Luppichini, M.; Bini, M.; Paterni, M.; Berton, A.; Merlino, S. A New Beach Topography-Based Method for Shoreline Identification. *Water* **2020**, *12*, 1–11. [CrossRef]
39. Chen, Z.; Muller-Karger, F.E.; Hu, C. Remote Sensing of Water Clarity in Tampa Bay. *Remote Sens. Environ.* **2007**, *109*, 249–259. [CrossRef]
40. Jiang, L.; Yan, X.; Klemas, V. Remote Sensing for the Identification of Coastal Plumes: Case Studies of Delaware Bay. *Int. J. Remote Sens.* **2009**, *30*, 2033–2048. [CrossRef]
41. Klemas, V. Remote Sensing of Coastal Plumes and Ocean Fronts: Overview and Case Study. *J. Coast Res.* **2012**, *28*, 1–7. [CrossRef]
42. Papakonstantinou, A.; Topouzelis, K.; Pavlogeorgatos, G. Coastline Change Detection Using UAV, Remote Sensing, GIS and 3D Reconstruction. In Proceedings of the Planning and Economics (CEMEPE 2015) and SECOTOX Conference, Mykonos Island, Greece, 14–18 June 2015.
43. Nunziata, F.; Buono, A.; Migliaccio, M.; Benassai, G.; Di Luccio, D. Shoreline Erosion of Microtidal Beaches Examined with UAV and Remote Sensing Techniques. In Proceedings of the 2018 IEEE International Workshop on Metrology for the Sea; Learning to Measure Sea Health Parameters (MetroSea), Bari, Italy, 08–10 October 2018; IEEE: New York, NY, USA, 2018. [CrossRef]
44. Vos, K.; Splinter, K.D.; Harley, M.D.; Simmons, J.A.; Turner, I.L. CoastSat: A Google Earth Engine-Enabled Python Toolkit to Extract Shorelines from Publicly Available Satellite Imagery. *Environmental Model. Softw.* **2019**, *122*, 104528. [CrossRef]
45. Vos, K.; Harley, M.D.; Splinter, K.D.; Simmons, J.A.; Turner, I.L. Sub-Annual to Multi-Decadal Shoreline Variability from Publicly Available Satellite Imagery. *Coast. Eng.* **2019**, *150*, 160–174. [CrossRef]
46. Gonçalves, D.; Gonçalves, G.; Pérez-Alvávez, J.A.; Andriolo, U. On the 3D Reconstruction of Coastal Structures by Unmanned Aerial Systems with Onboard Global Navigation Satellite System and Real-Time Kinematics and Terrestrial Laser Scanning. *Remote Sens.* **2022**, *14*, 1485. [CrossRef]
47. Scicchitano, G.; Scardino, G.; Monaco, C.; Piscitelli, A.; Milella, M.; De Giosa, F.; Mastronuzzi, G. Comparing Impact Effects of Common Storms and Medicanes along the Coast of South-Eastern Sicily. *Mar. Geol.* **2021**, *439*, 106556. [CrossRef]
48. Mentaschi, L.; Vousdoukas, M.I.; Pekel, J.-F.; Voukouvalas, E.; Feyen, L. Global Long-Term Observations of Coastal Erosion and Accretion. *Sci. Rep.* **2018**, *8*, 12876. [CrossRef] [PubMed]
49. Scardino, G.; Kushabaha, A.; Sabato, G.; Tarascio, S.; Scicchitano, G. Assessment of Medicane Helios Meteo-Marine Parameters Using a Machine Learning Approach. In Proceedings of the 2023 IEEE International Workshop on Metrology for the Sea; Learning to Measure Sea Health Parameters, MetroSea 2023, La Valletta, Malta, 4–6 October 2023; IEEE: New York, NY, USA, 2023; pp. 508–512.

50. Federici, P.R.; Mazzanti, R. *Note Sulle Pianure Costiere Della Toscana*; Italiana, S.G., Ed.; Società Geografica Italiana: Roma, Italy, 1993.
51. Mazzanti, R. *La Pianura Pisana e i Rilievi Contermini*; Società Geografica Italiana: Roma, Italy, 1994.
52. Sarti, G.; Bini, M.; Giacomelli, S. The Growth and the Decline of Pisa (Tuscany, Italy) up to the Middle Ages: Correlations with Landscape and Geology. *Quat. Ital. J. Quat. Sci.* **2010**, *23*, 311–322.
53. Sarti, G.; Bertoni, D.; Bini, M. Integrating Different Databases to Offer a Geological Perspective of Coastal Management: A Review Case from the Northern Tuscany Littoral Cell (Italy). *J. Mar. Sci. Eng.* **2022**, *10*, 353. [CrossRef]
54. Toniolo, A.R. Le Variazioni Storiche Del Litorale Toscano Fra l'Arno e Il Magra. In Proceedings of the Atti del X Congresso Geografico Italiano, Milan, Italy, 1 January 1927.
55. Toniolo, A.R. *Sulle Variazioni Di Spiaggia a Foce d'Arno (Marina Di Pisa) Dalla Fine Del Secolo XViii Ai Nostri Giorni: Studio Storico Fisiografico*; di Pisa, C., Ed.; Tipografia Municipale: Pisa, Italy, 1910.
56. Borgh, L. *Apporto Allo Studio Sulle Cause Di Variazione Del Litorale Pisano*; Topografia Comunale: Pisa, Italy, 1970.
57. Palla, B. Variazioni Della Linea Di Riva Tra i Fiumi Arno e Serchio (Tenuta Di S. Rossore—Pisa) Dal 1878 al 1981. *Atti Soc. Tosc. Sci. Nat., Mem. Serie A* **1983**, *90*, 125–149.
58. Bartolini, C.; Pranzini, E. Tracing Nearshore Bottom Currents with Sea-Bed Drifters. *Mar. Geol.* **1977**, *23*, 275–284. [CrossRef]
59. Luppichini, M.; Paterni, M.; Berton, A.; Casarosa, N.; Bini, M. Influences of the Ground Control Point (GCP) Configuration on the UAV-Derived Structure from Motion (SfM) in the Coastal Environment. *Earth Sci. Inform.* **2025**, *18*, 144. [CrossRef]
60. Lionello, P.; Özsoy, E.; Planton, S.; Zanchetta, G. Climate Variability and Change in the Mediterranean Region. *Glob. Planet. Change* **2017**, *151*, 1–3. [CrossRef]
61. Masselink, G.; Puleo, J.A. Swash-Zone Morphodynamics. *Cont. Shelf Res.* **2006**, *26*, 661–680. [CrossRef]
62. Eichentopf, S.; Karunarathna, H.; Alsina, J.M. Morphodynamics of Sandy Beaches under the Influence of Storm Sequences: Current Research Status and Future Needs. *Water Sci. Eng.* **2019**, *12*, 221–234. [CrossRef]
63. Uścinowicz, G.; Uścinowicz, S.; Szarafin, T.; Maszloch, E.; Wirkus, K. Rapid Coastal Erosion, Its Dynamics and Cause—An Erosional Hot Spot on the Southern Baltic Sea Coast. *Oceanologia* **2024**, *66*, 250–266. [CrossRef]
64. Trogu, D.; Buosi, C.; Ruju, A.; Porta, M.; Ibba, A.; De Muro, S. What Happens to a Mediterranean Microtidal Wave-Dominated Beach During Significant Storm Events? The Morphological Response of a Natural Sardinian Beach (Western Mediterranean). *J. Coast Res.* **2020**, *95*, 695–700. [CrossRef]
65. Enríquez, A.R.; Marcos, M.; Falqués, A.; Roelvink, D. Assessing Beach and Dune Erosion and Vulnerability Under Sea Level Rise: A Case Study in the Mediterranean Sea. *Front. Mar. Sci.* **2019**, *6*, 4. [CrossRef]
66. Delle Rose, M.; Martano, P. Wind–Wave Conditions and Change in Coastal Landforms at the Beach–Dune Barrier of Cesine Lagoon (South Italy). *Climate* **2023**, *11*, 128. [CrossRef]
67. Moraes, R.P.L.; Reguero, B.G.; Mazarrasa, I.; Ricker, M.; Juanes, J.A. Nature-Based Solutions in Coastal and Estuarine Areas of Europe. *Front. Environ. Sci.* **2022**, *10*, 829526. [CrossRef]
68. Davidson-Arnott, R. Waves—Wave Theory and Wave Dynamics. In Proceedings of the Introduction to Coastal Processes and Geomorphology; Davidson-Arnott, R., Ed.; Cambridge University Press: Cambridge, UK, 2009; pp. 78–115.
69. Valsamidis, A.; Reeve, D.E. A New Approach to Analytical Modelling of Groyne Fields. *Cont. Shelf Res.* **2020**, *211*, 104288. [CrossRef]
70. Nordstrom, K.F. *Beaches and Dunes of Developed Coasts*; Cambridge University Press: Cambridge, UK, 2000; ISBN 9780521545761.

Disclaimer/Publisher's Note: The statements, opinions and data contained in all publications are solely those of the individual author(s) and contributor(s) and not of MDPI and/or the editor(s). MDPI and/or the editor(s) disclaim responsibility for any injury to people or property resulting from any ideas, methods, instructions or products referred to in the content.